Spanish Journal of Agricultural Research
18 (4), e0209, 15 pages (2020)
eISSN: 2171-9292
https://doi.org/10.5424/sjar/2020184-15426
Instituto Nacional de Investigación y Tecnología Agraria y Alimentaria (INIA)

RESEARCH ARTICLE

OPEN ACCESS

Effects of fan volute structure on airflow characteristics in rice combine harvesters

Zhenwei Liang (Liang, ZW)[1,2], Depeng Li (Li, DP)[1], Jun Li (Li J)[1] and Kunpeng Tian (Tian KP)[3]

[1] *Jiangsu University, Key Laboratory of Modern Agricultural Equipment and Technology, Ministry of Education, Zhenjiang 212013, China.*

[2] *Wuxi Zhonghui Rubber Technology Co., Ltd, WuXi 214183,China* [3] *Nanjing Research Institute for Agricultural Mechanization, Ministry of Agriculture, Nanjing 210014, China.*

Abstract

Aim of study: Selecting a proper fan for the rice combine harvesters to get a good cleaning performance when harvesting high yield rice.

Area of study: Jiangsu Province, China.

Material and methods: Three potential multi-duct fans were designed, and the computational fluid dynamics and hot wire anemometer technology were utilized to learn the airflow and pressure variation inside the fan with perforated plates at the outlet ducts as cleaning loads. Then, the fan with the best performance was selected and a multi-duct cleaning test-bed was developed. The variation of the corresponding airflow velocity in the cleaning system was analyzed and the ideal airflow velocity in different section of the sieve was clarified. Finally, a field experiment was carried out.

Main results: For a rice combine harvester with a feed rate of 7 kg/s (material other than grain + grain), the requested airflow rates inside the cleaning shoe was about 3.0 m^3/s. The ideal airflow velocity in different section of the cleaning shoe was 8-9 m/s at upper duct, 4-6 m/s at the middle section, and 3-4 m/s at the tail section; large improvement in cleaning performance was achieved with the designed fan.

Research highlights: The airflow velocity decreased as the cleaning loads at the duct increased. The fan with the averaged airflow velocity ≥7 m/s at the upper duct under different cleaning loads, and the airflow velocity at the lowest duct ≥ 9 m/s, is favorable for forming a blowing airflow in the tail sieve and is good for grain stratification.

Additional key words: cleaning load; perforated plates; CFD; airflow distribution.

Abbreviations used: CFD (computational fluid dynamics); MOG (material other than grain)

Authors' contributions: Conceived and designed the study, performed the study, analyzed the data and wrote the manuscript: ZWL. Critically revised the manuscript and polished the expression: DPL, JL, KPT.

Citation: Liang, ZW; Li, DP; Li J; Tian KP (2020). Effects of fan volute structure on airflow characteristics in rice combine harvesters. Spanish Journal of Agricultural Research, Volume 18, Issue 4, e0209. https://doi.org/10.5424/sjar/2020184-15426

Received: 07 Jul 2019. **Accepted:** 20 Nov 2020.

Funding agencies/institutions	Project / Grant
National Natural Science Foundation of China	51905221
Natural Science Foundation of Jiangsu Province, China	BK20190859
China Postdoctoral Science Foundation	2019M651746&2020T130260
The Natural Science Foundation of the Jiangsu Higher Education Institutions of China	19KJB210009
Synergistic Innovation Center of Jiangsu Modern Agricultural Equipment and Technology, China	4091600027
Jiangsu Province Postdoctoral Foundation for researchers, China)	2019Z106
Jiangsu Association of Science and Technology Young Talent Support Project	2020-21
Priority Academic Program Development of Jiangsu Higher Education Institutions, China	PAPD-2018-87

Competing interests: The authors have declared that no competing interests exist.

Correspondence should be addressed to Zhenwei Liang: liangzhenwei518@126.com

Introduction

It is reported that the super rice planting area has risen to 9.067 million ha, accounts for approximately one-third of total crop planting area in China and the average rice yield climbs to 11250 kg/ha per harvesting (Yuan, 2017). However, the currently used combine harvesters in China were designed according to rice with a yield ≤ 9000 kg/ha,

and field experiment results indicated that those combine harvesters have poor cleaning performance when harvesting high yield rice (Li & Li, 2015). Thus, it is necessary to upgrade the cleaning section of the combine harvester to adapt it to high moisture and high yield conditions. Relevant research on cleaning structural improvement has been carried out: using Particle Image Velocimetry (PIV) system to analyze the airflow distribution in the cleaning system (Kenney *et al.*, 2005); connecting the aerofoil and centrifugal blades together and expecting to suit for the threshed outputs distribution (Tang *et al.*, 2007). The trajectories of the threshed soybean grains in the classifier chamber were recorded by a high-speed camera to investigate the effect of grain movement on cleaning performance (Adewumi *et al.*, 2008). A conical centrifugal fan was designed to adjust threshed output initial distribution on the sieve surface, and the cleaning performance was improved significantly in the transversal axis-flow combine harvester (Chen *et al.*, 2009). To make clear airflow turbulent flow characteristics and its passage through the grains, the cleaning airflow velocity was measured by PIV and Laser Doppler Velocimetry (Ueka *et al.*, 2012). A high power centrifugal fan with six blades was utilized in TC5060 axial-flow combine harvesters (New Holland), and field experiment results indicated that the cleaning system could spread the threshed outputs promptly, and the cleaning performance was improved with a stronger airflow power (Wu, 2014). On the other hand, two single-duct centrifugal fans were utilized in YANMAR YH880 series combine harvesters. Some multi-duct fans also has been used in some flagship combine harvesters, such as Gleaner S8 combine harvester.

From these experiments, it can be learnt that the development of the harvesting machinery mainly follows the structural design, field test validation and structure optimization. Apparently, such a method is seriously affected by the harvesting seasons, the development cycle is generally long and seriously hinders the rapid progress in industry technology. With the development of the computation science, the agriculture machinery development cycles has been shortened significantly (Zhao *et al.*, 2018; An *et al.*, 2020), as the airflow velocity measurements only provide limited information and would have to be repeated for every new configuration of the cleaning section, computational fluid dynamics (CFD) simulations has been widely used for cleaning system structural optimization in the past years (Dilin *et al.*, 1998; Muggli *et al.*, 2002; Kenney *et al.*, 2005; Kergourlay *et al.*, 2006; Gebrehiwot *et al.*, 2010a; Casarsa & Giannattasio, 2011; Xu *et al.*, 2015). However, most of this structural optimization use CFD simulation without taking cleaning loads into consideration. In this paper, a proper cleaning system for a rice combine harvester with a feed rate of 7 kg/s was developed by considering effect of cleaning loads on airflow distribution.

Material and methods

Fan geometric models under consideration

The total airflow rate V (m^3/s) generated by a fan is an important performance criterion. The total airflow volume rate V is determined by the amount of material other than grain (MOG) in the threshed output and can be calculated by the following equation (Chinese Academy of Agricultural Mechanization Sciences, 2007):

$$V = \frac{\beta Q}{\mu \rho} \quad (1)$$

where β is the ratio of the MOG in the total threshed outputs (typically 10%-15%), Q is the feed rate (Grain + MOG) in kg/s, ρ is the airflow density (1.225 kg/m) and μ is 0.2-0.3.

For a combine harvester with a feed rate of 7 kg/s, the requested airflow rates inside the cleaning shoe can be calculated by Eq. (1) with β=14%, ρ=1.225, μ=0.25. This indicates that under these assumptions, an airflow rate of 3.0 m^3/s is required for good cleaning performance. To analyze the effect of the flow channel shape of the upper outlet on the inner flow field distribution, three models with different φ, R_5, L and H were developed based on an existing single-duct fan (Li & Li, 2015). Apart from compression stroke φ, horizontal dimension L, and vertical dimension H, all three fans have the same number of blades and internal diameter. For Fan I: φ=89°, L=27.1 mm, H=205.8 mm, and R_5=208.7 mm; for Fan II: φ=97°, L=27.1 mm, H=205.8 mm, and R_5=232.5 mm; Fan III: φ=121°, L=129.8 mm, H=164.5 mm, and R_5=232.5 mm. The geometry of the designed fan is shown in Fig. 1.

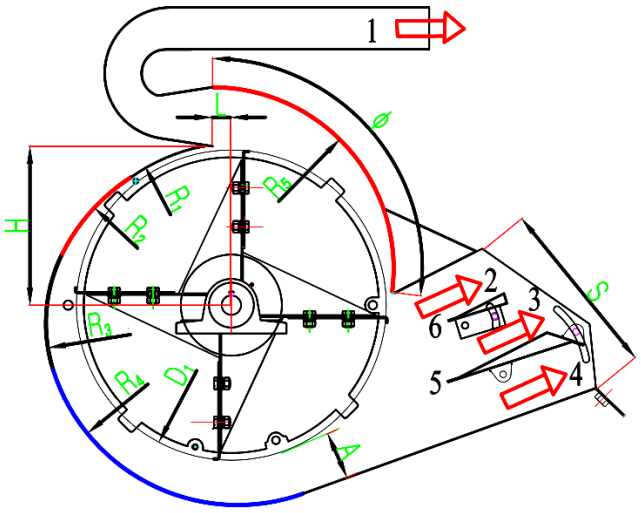

Figure 1. Schematic diagram of the multi-duct fan: 1, 2, 3 and 4, ducts 1, 2, 3 and 4, respectively; 5 and 6, guide plates I, and II, respectively.

CFD simulation and results validation

A literature review has indicated that the resistance value of a cleaning load at fan outlets can be calculated from the deduced fluidized grain resistance model and the airflow resistance model (Molenda *et al.*, 2005; Gebrehiwot, 2010; Liang *et al.*, 2020). Perforated plates with different circular hole layouts were designed and placed on fan outlets to represent cleaning loads. The perforated plates were set as porous media, and the porous coefficients for different working loads were acquired by wind tunnel setup experiments (Gebrehiwot *et al.*, 2010b). ICEM-CFD 15 software (ANSYS Inc, Canonsburg, PA, USA) was utilized as the grid generation tool, and the grid numbers for different parts in the fan models are listed in Table 1. It is indicated that steady calculations for fan rotation can cause significant calculation errors (Xu *et al.*, 2015), and compared with the multiple reference frame (MRF) and the mixing plane model, the sliding mesh method assumes that the flow field is unsteady, and the flow field variation in both time and space, specifically in the circumferential direction, is fully considered in the transient sliding mesh methodology (Dieter *et al.*, 2005). Therefore, in this work the blade-volute interaction was modeled by the sliding mesh technique (Seo *et al.*, 2003). In the calculation, the blade domain was defined as a moving zone, while the volute and inlets were defined as stationary zones. The operating pressure was set to 101,325 Pa. The rotational speed of the fan blades was 1300 rpm, the boundary condition for the inlets was set as a pressure inlet of 0 Pa, while the lower outlet was set as a pressure outlet of 0 Pa, and the time step was 2.56×10^{-4} s (Sakya *et al.*, 1993; Semion *et al.*, 2003; Gao *et al.*, 2018). Apart from Newton's equation and Naiver-Stokes equations, the realizable k-ε turbulence model was used in the CFD simulation to calculate the mean flow characteristics for turbulent flow conditions and describe the turbulent properties inside the fan. Meanwhile, in selecting the least squares cell-based gradient as the gradient discretization method, the second-order upwind scheme was adopted as the momentum equation, the second-order upwind scheme was adopted to calculate the turbulent dissipation rate, the second-order upwind scheme was adopted as the turbulent kinetics, and the first-order implicit scheme was used to calculate the transient formulation (Zhang *et al.*, 2018). The major concern with multi-duct fans is the required air distribution for different ducts. Apart from the evenly distributed airflow velocity at the ducts, a good fan should also be able to push the airflow passing the fan ducts with a reasonable air flow ratio, which means that the total pressure-volume curve for the best fan should have a steep slope. A fan outlet airflow velocity measurement system were developed to validate the simulation results, as shown in Fig. 2.

With the selected fan, a cleaning test bed was developed, and the cleaning experiment was conducted in the cleaning test bed. Meanwhile, the corresponding airflow velocities were measured by the VS110 anemometer in the cleaning section. The measurement point distribution is shown in Fig. 3, and the distance of each measurement point was 180 mm.

Finally, field experiments were conducted in Wujiang, Suzhou city, China. The combined harvester advance velocity was 1-1.2 m/s to guarantee a feed rate of 7 kg/s (Grain + MOG). The method used to evaluate the overall harvesting performance can be found in our previous publication (Liang *et al.*, 2019). The properties of the harvested rice were as follows: the average spike length was 14-16 mm; the average yield, 11150.6 kg/ha; thousand seed mass, 27~31g; average straw moisture content, 72.3%; average grain moisture content, 25.1%; average MOG/Grain ratio, 2.24.

Table 1. Grid number for different parts in different fan models

Location	Number of grid		
	Model I	Model II	Model III
Volute	6586644	4753042	10384728
Inlet zone	64908	64908	64908
Blade zone	4096540	4096540	4096540
Outlet 1	178332	178332	178332
Outlet 2	182584	182584	182584
Outlet 3	157228	157228	157228
Outlet 4	132671	132671	132671

Results and discussion

CFD simulation result validation by airflow velocity measurement

The equivalent cleaning resistance is 0.16-3.52 for the upper outlet and 0.95-6.10 for the lower outlet in the case of a cleaning system with feeding rates of 0-4 kg/s based on the deduced fluidized grain resistance model and the airflow resistance model (Molenda *et al.*, 2005; Gebrehiwot, 2010; Liang *et al.*, 2020). A comparison of the simulated and measured airflow velocities with resistances of 0 and 2.19 at the ducts is shown in Fig. 4. In Fig. 4, the range of the root mean square errors (RMSEs) of the measured and simulated airflow velocity was distributed from 0.12 to 0.46 m/s. It is indicated in Fig. 4 that the distance between the measurement results and the simulated airflow velocities was ≤ 15% at the four ducts, and the error was much greater at certain points near the duct

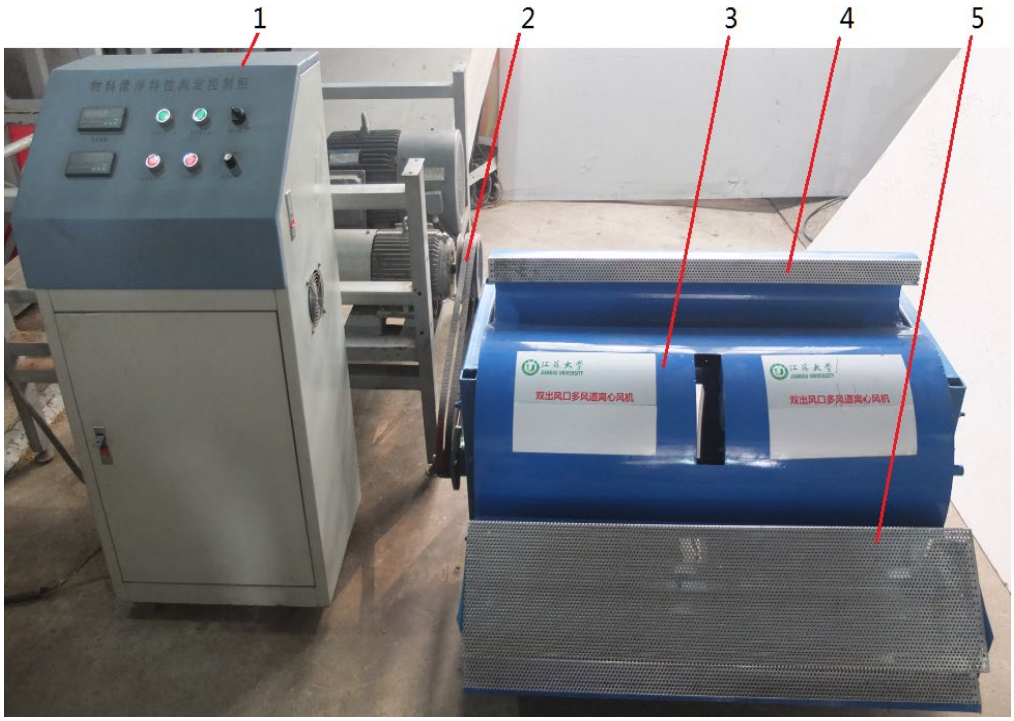

Figure 2. 1, control cabinet; 2, motor; 3, fan; 4, perforated plates at upper duct; 5, perforated plates at lower duct.

sides. Such an error of magnitude is considered good, as the airflow anemometer can only obtain airflow velocity values in one dimension at each measurement point, and it is difficult to determine the airflow direction inside the cleaning shoe with the airflow anemometer. This is one of the sources of the measurement error. On the other hand, there are some errors in the manufacturing process; for example, the fan volute was based on the Archimedes spiral, and the volute was composed of four arcs with radii R_1, R_2, R_3 and R_4. The compression stroke may not be as accurate in the manufacturing process as in the CFD simulation, resulting in a calculation error. Compared with the simulation results reported by Gebrehiwot *et al.* (2010a), in which the distance between the measured and the simulated value is within ± 25%, errors ≤ 15% can be considered acceptable.

In Fig. 4a, as there is a larger resistance during airflow transport from duct 4 to the tail sieve, the airflow velocity was generally ≤ 12 m/s at duct 4 of Fan I, and the airflow always diffused to places with a lower resistance after leaving the fan ducts. The airflow from duct 4 may not be sufficient for the tail sieve after continuous attenuation. In this case, the short straw in the tail sieve section would enter the tail auger, thus negatively affecting the cleaning efficiency. Fig. 4b shows that the airflow velocity from duct 4 of Fan II was in a range of 15-17 m/s, and the airflow velocity was distributed in the range of 10-13 m/s from duct 1. The airflow velocity distribution was

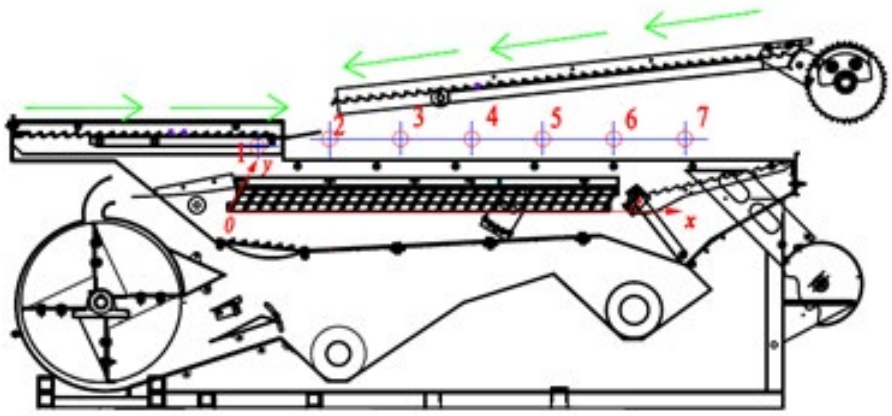

Figure 3. Airflow velocity measurement distribution in the cleaning test-bench.

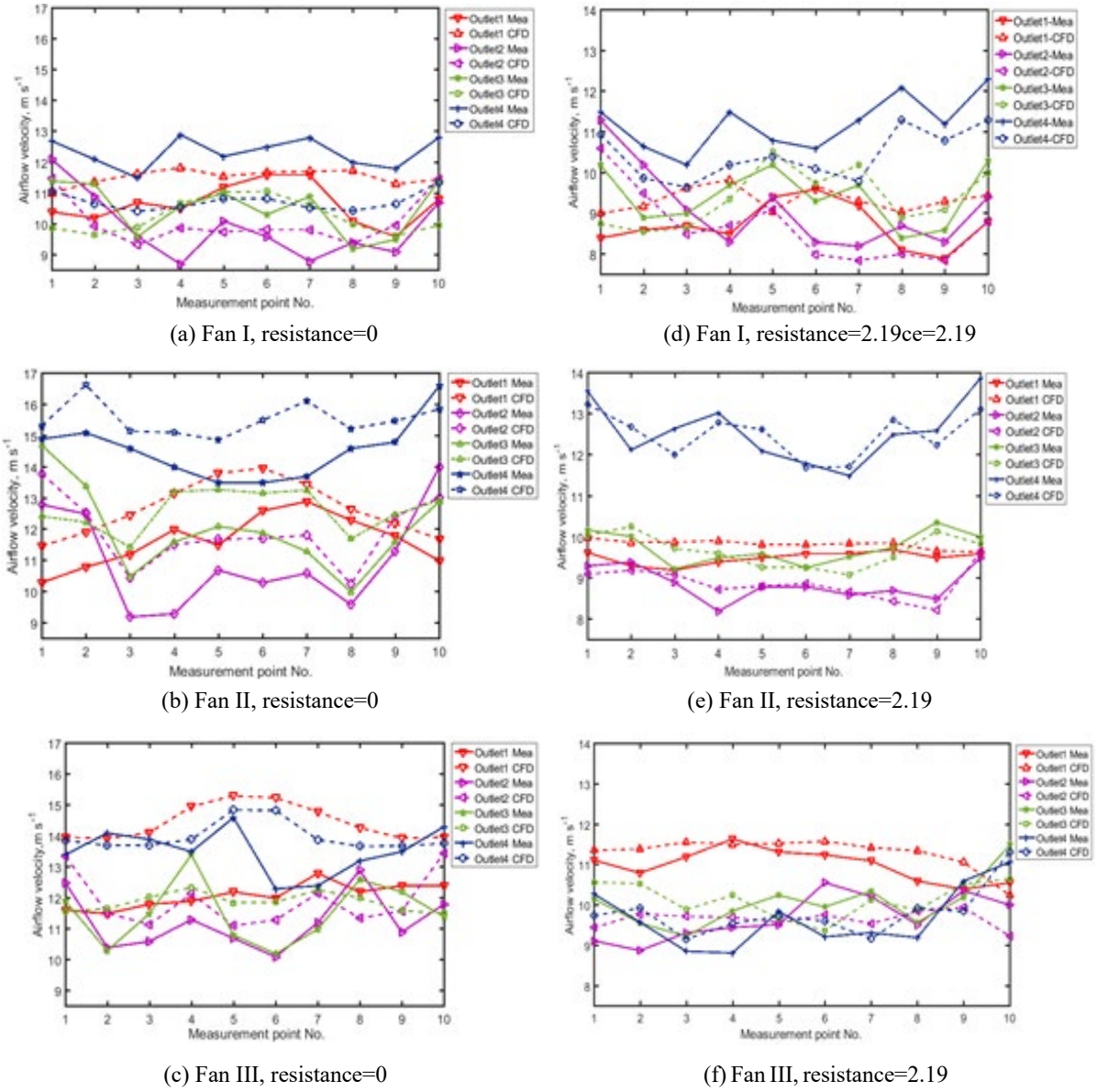

(a) Fan I, resistance=0 (d) Fan I, resistance=2.19ce=2.19

(b) Fan II, resistance=0 (e) Fan II, resistance=2.19

(c) Fan III, resistance=0 (f) Fan III, resistance=2.19

Figure 4. Measured and simulated airflow velocity at ducts with the corresponding guide plate I angle 29°, guide plate II angle 27°and fan speed 1300 rpm.

generally more balanced at all the ducts of Fan II. Fig. 4c shows that for Fan III, the airflow velocity from duct 4 experiences a large fluctuation in the center of the duct in the traverse direction, which is not beneficial to cleaning. Figs. 4d,e,f indicate that the airflow velocity decreased as the cleaning load at the duct increased. In conclusion, Fan II can be expected to achieve good cleaning performance.

Variation of airflow inside the fans under different cleaning load

Fan I. Fig. 5a shows that the airflow inside the fan volute is sucked into the volute casing along the fan axis direction, and the inhaled air flows along the circumferential direction gradually during the fan blade rotation. The airflow velocity increases in the blade radial direction, and the maximum value is reached at the outer circle of the fan blades. As the fan blades rotate from the volute tongue (point A) to point B, the cross-sectional area gradually decreases, the partial kinetic energy of the fan blade is converted into airflow kinetic energy, the airflow velocity increases gradually, and part of the airflow is diverted into the upper duct in this process. As the fan blade keeps moving to point B, the airflow velocity increases dramatically as the cross-section decreases. After the blades pass through point B and the cross-section increases gradually, the radial resistance from the volute casing weakens, and the airflow velocity increases further. The air flows along the volute casing line and is guided to

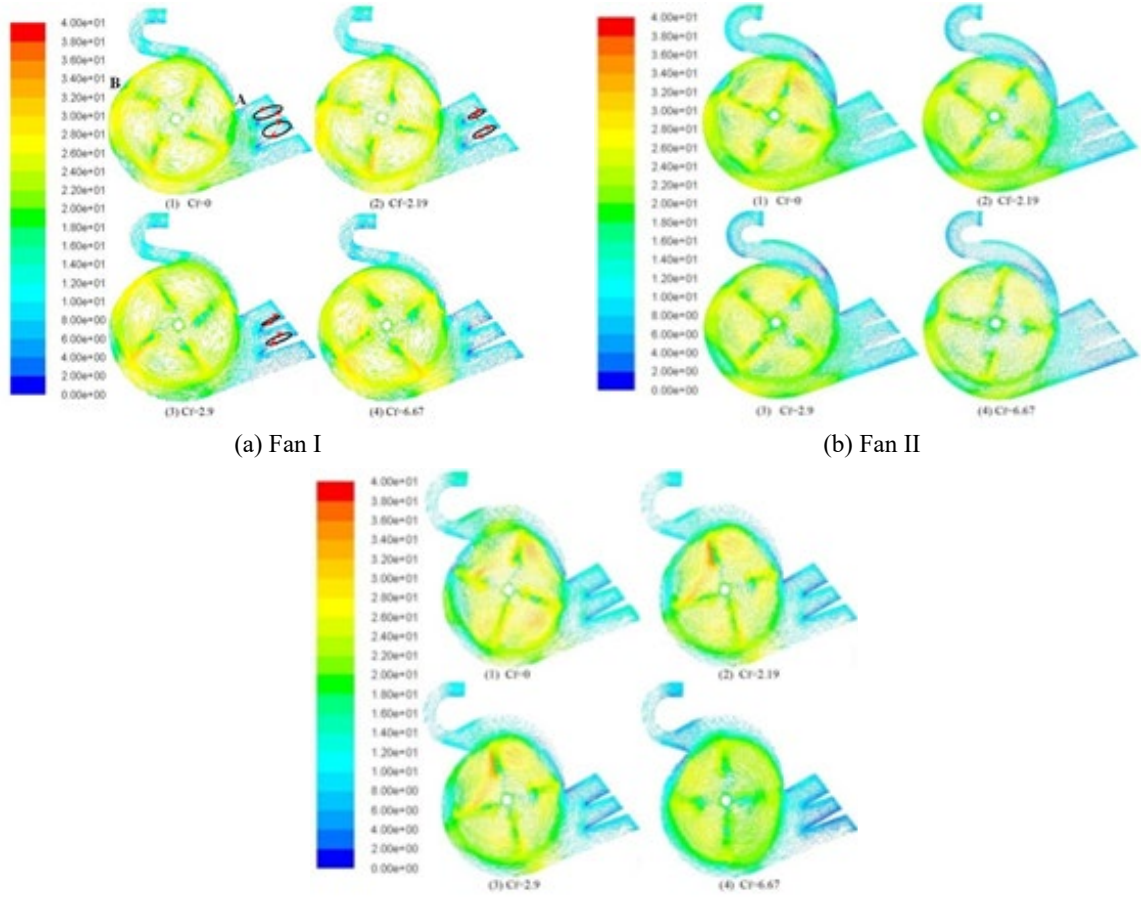

(a) Fan I

(b) Fan II

(c) Fan III

Figure 5. Velocity vector plot under different cleaning load inside the fan

the end of the spiral casing line. The airflow is routed into the three ducts in the lower outlet by guide plates. There are some eddy currents present in the lower edge of duct 2 and duct 3, which result in some energy loss. As the load increases (higher resistance values), the eddy scope and the airflow velocity inside the fan gradually decrease, resulting in a reduced airflow velocity at each duct.

Fig. 6a indicates that the cleaning load has a significant effect on the airflow velocity distribution at ducts 2 and 3. The minimum value is only 5.3 m/s, resulting in a relatively small airflow velocity in the middle sieve section, where the MOG could not be effectively separated from the grains. The airflow velocity at duct 4 is also lower under different cleaning loads, and the MOG can enter the tailing auger and affect cleaning efficiency. The airflow velocity is uniform at the ducts and also affects the cleaning performance. From the velocity distribution contour plots at the Fan I ducts, there is an even distribution of airflow velocity magnitude in the width direction of duct 2 and duct 3, while the airflow velocity at duct 1 and duct 4 experiences a notable fluctuation in the width direction.

Fan II. A velocity vector plot inside the fan under different cleaning loads for Fan II is shown in Fig. 5b and indicates that the velocity has increased for the airflow from duct 1 of Fan II compared with duct 1 of Fan I. The airflow flow is smooth, and the airflow velocity is ideal at the ducts. There is also no eddy at the ducts, which is helpful for obtaining good cleaning performance. The variation of airflow status in the ducts under different cleaning loads for Fan II shown in Fig. 6b indicates that there is a slight difference in terms of airflow volume for ducts 1, 2, and 3, and the greatest airflow volume occurs at duct 4. The cleaning load has little influence on the airflow velocity of duct 1. The averaged airflow velocity is ≥7 m/s at duct 1 under different cleaning loads, which is beneficial for pre-cleaning, and the airflow velocity at duct 4 is ≥ 9 m/s, which is favorable for forming a blowing airflow in the tail sieve. The airflow contour plots indicate that the airflow from duct 1 is more evenly distributed, which is good for grain stratification.

Fan III. The internal airflow velocity plot of Fan III shown in Fig. 5c indicates that the internal airflow velocity is higher, and the airflow volume at duct 4 declined notably as the working load increased. As the airflow from duct 4 mainly covers the middle and rear parts of the cleaning sieve, a small airflow volume leads to a larger portion of short straw falling into the grain auger. Meanwhile, the probability of short straws entering

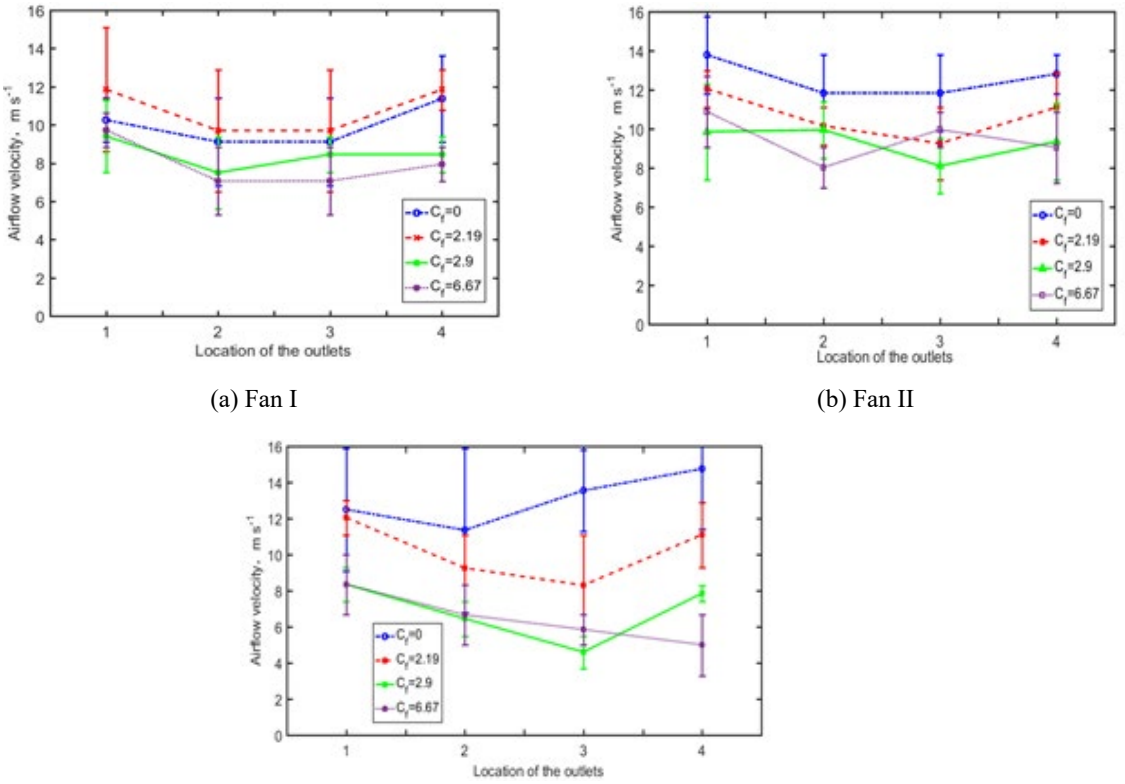

(a) Fan I

(b) Fan II

(c) Fan III

Figure 6. Variation of airflow velocity at the fan ducts

the tail auger increases. Fig. 6c shows the variation of airflow volume rates in ducts under different cleaning loads for Fan II. The airflow velocity and the airflow volume rates at the ducts decrease with increasing cleaning load, and the airflow volume rate decrease when ducts with an equivalent resistance of 0-2.9 are larger than ducts with an equivalent resistance of 2.9-6.67. The cleaning load has the greatest effect on the airflow velocity at ducts 3 and 4, and the minimum airflow velocity is only approximately 3 m/s, which is close to the suspension velocity of short straws, and the short straw will enter the tailing auger and affect cleaning efficiency. From the velocity contour plots at the ducts of Fan III, we can see that there is an even distribution of airflow velocity at ducts with a zero cleaning load. With increasing cleaning load, the airflow velocity value along the duct width is not even, and the airflow velocity on the left side of the duct is higher than that on the right side, which is not conducive to forming a reasonable airflow field in the cleaning shoe. Therefore, Fan III is not suitable for high cleaning load conditions.

Comparison of airflow volume at ducts under different cleaning loads

The airflow volume rates in the ducts of the different fans are shown in Fig. 7 for the different equivalent cleaning loads. Fig. 7d shows that Fan II generates the largest airflow volume rate, while Fan I is the smallest for an equivalent cleaning load of 6.67. Compared to Fan II, the airflow volume in duct 4 of Fan I and Fan III is relatively small, which is not good for forming an upward airflow at the tail sieve to separate the short straw instantly. Therefore, Fan I and Fan III are not suitable for high cleaning load occasions. However, the airflow volume rate in duct 3 of Fan II is smaller at higher cleaning load conditions, which is not conducive to rapid grain dispersion and penetration in the sieve middle section, and the probability of straws entering the grain auger is increased. To obtain a better cleaning performance under high cleaning load conditions, the fan speed should be increased to upgrade the airflow velocity from duct 1; thus, the initial grain dropping points can be located in the airflow covering area from duct 2, and the sieve opening can be reduced moderately. Meanwhile, a backward airflow is formed, and short straws are removed quickly under acceleration of the airflow from duct 4. From the airflow volume rates in the different ducts with equivalent cleaning loads in the 0-2.9 range, Figs. 7a,b,c show that the airflow volume rate increases gradually as the cleaning load decreases. Moreover, Fan II shows the largest increase in the airflow volume rate. In addition, the airflow distribution in ducts 1, 2 and 3 of Fan II is more balanced.

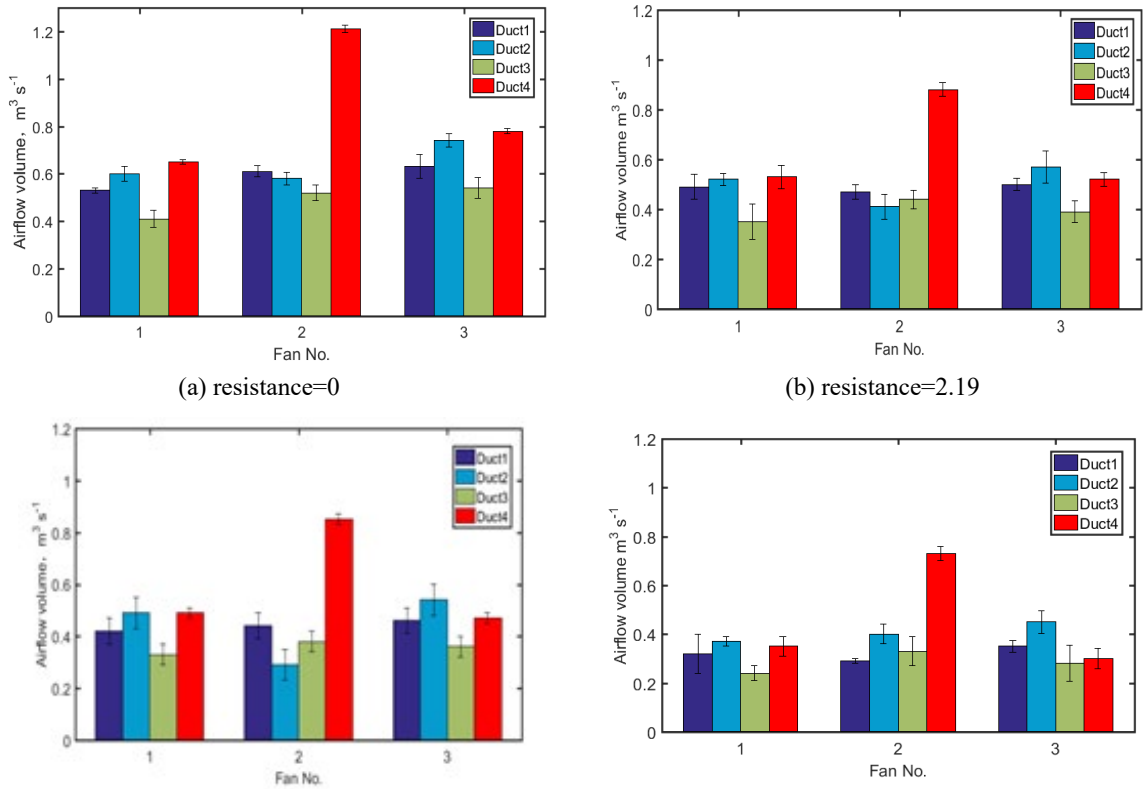

Figure 7. Variation of the airflow volume at fan ducts with a guide plate I angle of 29°, guide plate II angle of 27°, fan revolution speed of 1300 rpm different cleaning loads

Effect of volute casing structure on pressure characteristics

From the general fan pressure characteristic curves of the three fans through the CFD simulation shown in Fig. 8, Fan I fulfills the requirement for a steep pressure characteristic at each duct. However, the total airflow rate is only 2.2 m^3/s, which is lower than the target rate of 3.0 m^3/s. The total airflow volume rate for Fan III is only 2.61 m^3/s. Moreover, although there is a good pressure performance exhibited in ducts 1, 2 and 3, the airflow volume rate at duct 4 decreases greatly with increasing loading. The total airflow volume rate generated by Fan II is 2.92 m^3/s, which is very close to the target value. Moreover, Fan II exhibits good pressure characteristics at different cleaning loads for all 4 ducts. In conclusion, Fan II is the most suitable for implementation in the cleaning part of the combine harvester.

Comparison of total pressure at ducts for different loads

Pressure contour plots of fans at different loads are shown in Fig. 9. With the increase of the cleaning loads at the ducts of Fan II, the total pressure increased accordingly; this is beneficial to grain dispersion and upgrades the cleaning efficiency. However, for the other two fans, the response of the total pressure to the increasing loads was more variable, especially for Fan III. As the cleaning load increased, the total pressure in duct 1 and duct 4 decreased. This is not desirable because the pressure cannot disperse the higher amount of threshed outputs responsible for the increased load. Therefore, Fan III is not suitable for higher load conditions.

Variation of airflow distribution at each duct of Fan II

Previous research has indicated that fan speed greatly affects cleaning performance. A higher fan speed typically leads to a lower grain impurity ratio, but a fan speed that is too high results in an increase in grain sieve losses. It has also been shown that the guide plate angle has an effect on the cleaning performance by redistributing the airflow over the sieves. To obtain more insight into the variation in airflow distribution at each duct of Fan II under different fan speeds, guide plate angle combinations were performed using CFD simulations. In this paper, the four ducts were subjected to an equivalent working load of 6.67 to simulate the most extreme working conditions.

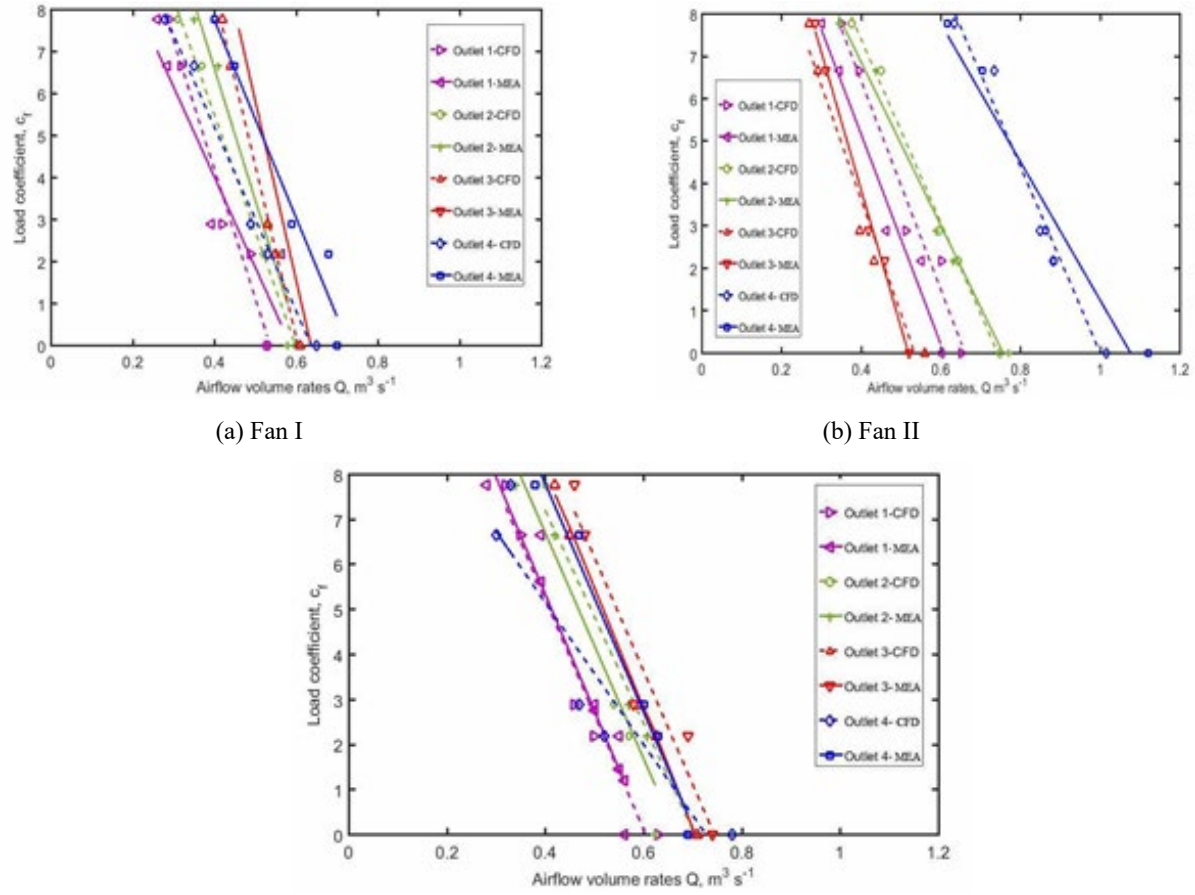

(a) Fan I

(b) Fan II

(c) Fan III

Figure 8. Performance curves for different fans. MEA: measurement value

(1) Effect of fan speed. The upper and lower outlets of the fan with four ducts play different roles. Therefore, the effect of fan speed on the airflow volume rate should be quantified for the different ducts. In Fig. 10, the variation in airflow volume rate as a function of the fan speed is illustrated for the four ducts subjected to an equivalent working load of 6.67. When the fan speed was increased from 1100 rpm to 1500 rpm, the generated total airflow volume rate rose from 1.3 m^3/s to 1.8 m^3/s. Fan speed had the largest effect on the airflow volume rate through duct 4, where the corresponding airflow volume rate increased from 0.49 to 0.73 m^3/s, compared to an increase from 0.288 to 0.40 m^3/s for duct 1.

The simulated velocity vectors inside the fan illustrated in Fig. 11 indicate that the internal airflow velocity increased gradually as the fan speed increased. With the increase in fan speed, the airflow velocity at the end of the spiral casing line also increased. This is because the kinetic energy of the gas molecules increased significantly as the airflow rotates in the volute. The airflow is guided towards the end of the spiral casing line, and the accelerated airflow is ejected from duct 4, resulting in a significant increase in the airflow velocity at duct 4. Moreover, the increase in airflow speed through the upper duct with increasing fan speed subjects the grain and MOG entering the cleaning shoe to greater acceleration in the direction of the back of the cleaning shoe. A fan speed of 1500 rpm and a working load of 6.67 resulted in an airflow velocity from the upper duct of approximately 8 m/s. This high air speed is expected to blow the rice grains towards the back, which may increase sieve losses. Therefore, a fan speed below 1500 rpm is recommended in most cases to maintain a reasonable grain sieve loss ratio level.

(2) Effects of guide plate angle

a) Guide plate I. The variation in airflow volume rate through each duct as a function of the guide plate angle is illustrated in Fig. 12. When the guide plate I angle was increased from 18° to 45°, the total airflow volume rate was reduced from 2.18 to 1.34 m^3/s. The airflow volume at duct 3 decreased with an increase in the guide plate I angle from 30° to 45°, resulting in a relatively low airflow velocity in the middle section of the sieve. This is not beneficial for the penetration of the threshed mixture and might lead to a larger grain impurity ratio in the grain tank. The airflow volume at duct 1 and duct 2 shows a trend of first increasing and then decreasing

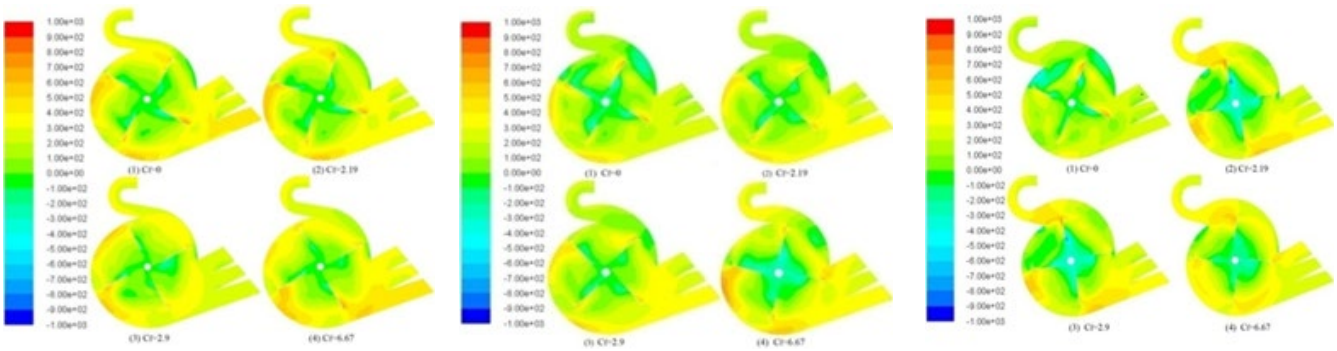

(1) Fan I (2) Fan II (3) Fan III

Figure 9. Total pressure contours of different fans under different cleaning loads.

with an increase in the guide plate I angle. The airflow volume at duct 4 reached its maximum value when the guide plate I angle was 30°. The velocity vector inside the fan under different guide plate I angles is shown in Fig. 13.

Figs. 13a,b,c show that the airflow velocity inside the fan decreased as the guide plate I angle increased. Duct 2 received the smallest airflow velocity in the case of a guide plate I angle of 30°. The guide plate I angle had a paramount influence on the airflow velocity at duct 3, and the corresponding airflow velocity decreased with increasing guide plate I angle. Therefore, it is better to keep guide plate I at a small angle in combine harvesters.

b) Guide plate II. The effect of the guide plate II angle is also visualized in Fig. 12. As the angle of guide plate II is increased from 18° to 45°, the generated total airflow volume rises from 1.6 to 1.76 m^3/s and then basically remained the same. The guide plate II angle had a marginal effect on the airflow volume rates at ducts 1 and 4 but a large effect on the airflow volume rate at ducts 2 and 3. The volume rate at duct 2 stays more or less constant when the guide plate II angle was increased from 18° to 30° but decreased from 0.40 m/s to 0.23 m/s as the guide plate II angle is further increased from 30° to 45°. The volume rate at duct 3 increased from 0.16 to 0.43 m^3/s as the guide plate II angle was increased from 18° to 45°. The variation in airflow velocity inside the fan with different guide plate II angles is shown in Figs. 13e,f,g, where with the increase in the guide plate II angle, the airflow velocity inside the fan rose at first and then decreased. At the same time, the airflow from duct 1 was distributed in a layered status, and the airflow velocity was distributed in the range of 7-10 m/s, thus providing a better pre-cleaning function. The averaged airflow velocity at ducts 2 and 3 was the smallest when the guide plate II angle was 30°. However, in the case of guide plate II with a small angle, the airflow at duct 2 experienced an uneven distribution, and it was easy to produce a cyclone in the cleaning shoe; this is not beneficial for the threshed outputs to obtain a continuous airflow effect. Changing the guide plate II angle had no effect on the airflow velocity at duct 4.

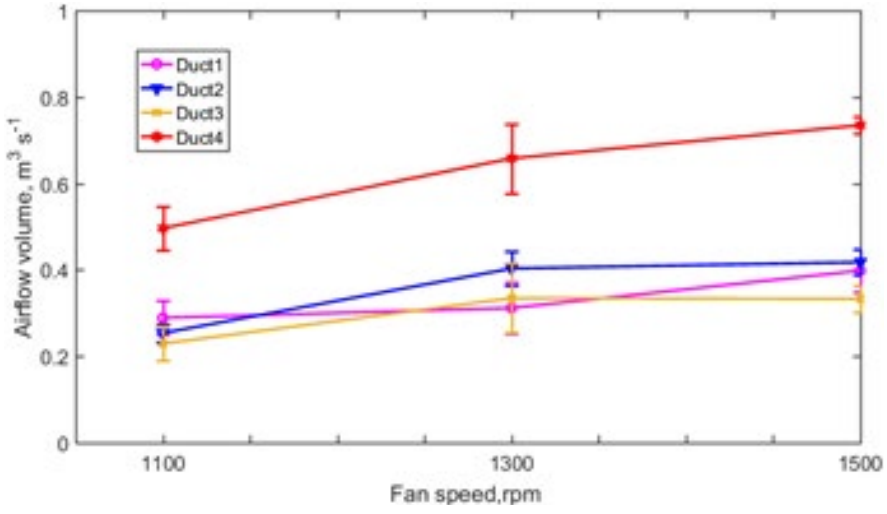

Figure 10. Airflow volume for Fan II with different speeds with an equivalent working load of 6.67

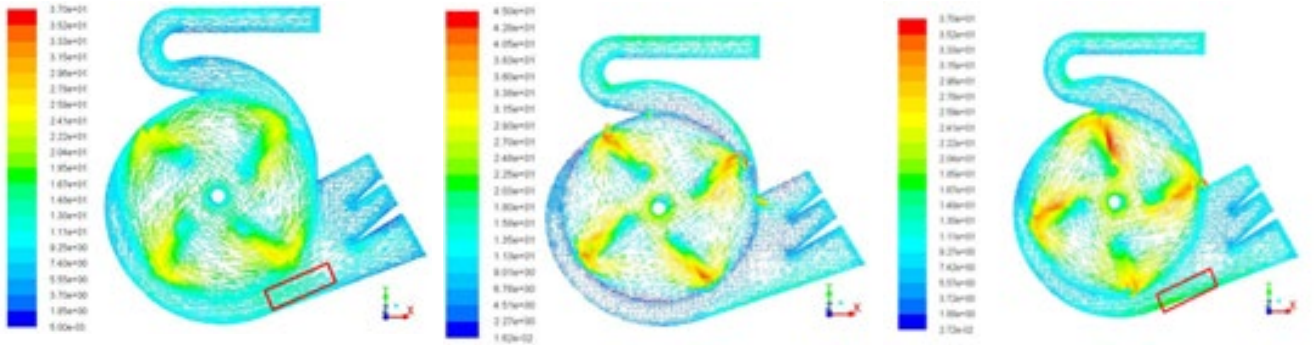

(a) 1100 rpm (b)1300 rpm (c)1500 rpm

Figure 11. Velocity vector inside the fan under different fan revolution speed with an equivalent working load of 6.67

In conclusion, the cleaning system can achieve good cleaning performance with the following parameters: fan speed: 1100-1300 rpm, guide plate I angle ≤ 18° and guide plate II angle 30-45°.

Cleaning performance and the corresponding airflow velocity variations

The cleaning experiment results with a feed rate of 2.5 kg/s under different working parameters indicated in Table 2, which shows that the developed cleaning device had a good cleaning performance compared with the conventional single duct cleaning device (Li & Li, 2015). The airflow velocity variation under different conditions with a feeding rate of 2.5 kg/s is shown in Fig. 14.

— Under test 1 in Fig. 14a, the maximum airflow velocity from the fan upper duct could reach 12.25 m/s. However, the airflow velocity was not uniform in its width direction; the distance between the maximum and the minimum value was 4 m/s, and the airflow velocity was much higher at the middle than at the edges. As the averaged airflow velocity was ~ 10.5 m/s, the light impurities could be blown out instantly, and the cleaning load could be reduced significantly. Then, the airflow velocity was reduced gradually along the sieve length and recovered to some extent at the tail sieve. However, the airflow velocity was slower, in a range of 360-720 mm, and the grain impurity ratio increased.

— Under test 2 in Fig. 14b, the airflow velocity from the upper duct was more uniform in the transverse direction of the fan, and the corresponding airflow velocity was distributed from 7.24 to 8.7 m/s, almost equal to the suspension speed of the rice grain. Although light impurities could be separated instantly, the airflow was not sufficient to keep the grains in the fluidized status in the cleaning shoe, which could lead to threshed output accumulation in the sieve front section. The airflow velocity was generally low, at 540-900 mm of the sieve length direction, and the straw entered the grain tank, resulting in a high grain impurity ratio.

— Under test 3 in Fig. 14c, the airflow velocity at the fan upper duct was more even in the transverse direction, and the averaged airflow velocity was distributed at ~ 9.7 m/s. The airflow velocity decreased in the 0-180 mm sieve length direction, the grain falling into the sieve could be dispersed rapidly, and the cleaning efficiency increased correspondingly.

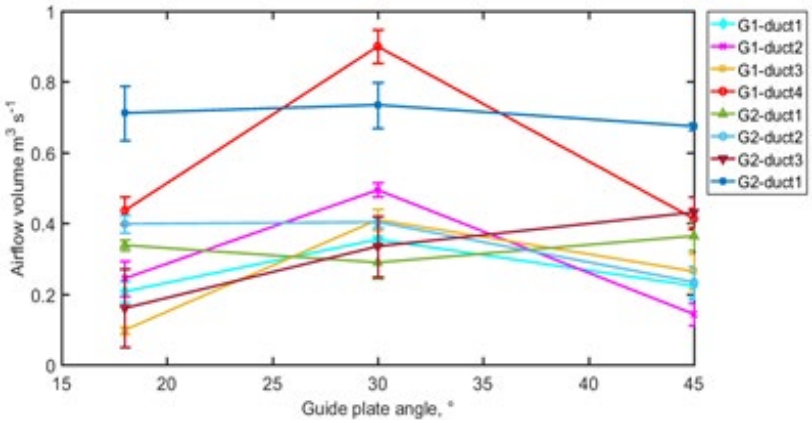

Figure 12. Variation of airflow volume at each duct with different guide plate angles for an equivalent working load of 6.67

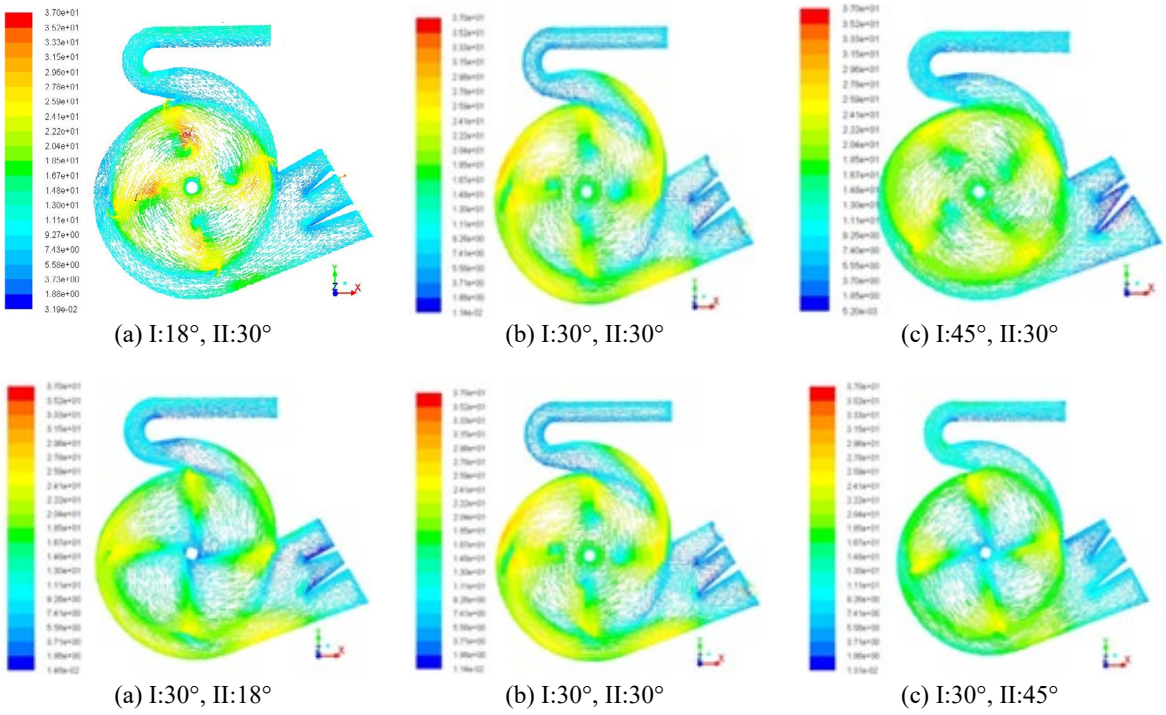

(a) I:18°, II:30° (b) I:30°, II:30° (c) I:45°, II:30°

(a) I:30°, II:18° (b) I:30°, II:30° (c) I:30°, II:45°

Figure 13. Variation of airflow velocity inside the fan with different guide plate angles

— Under test 4 in Fig 14d, the airflow velocity distribution was more reasonable. The airflow velocity increased to 4-5 m/s at a sieve length of 360 mm, which is beneficial to grain dispersion and penetration. Most of the short straws were transported to the tail sieve, and the straw had a small probability of entering the grain auger; the grain impurity ratio was lower. At the tail sieve, the airflow velocity rapidly rose, and the corresponding airflow velocity could reach 5.77 m/s. The short straw could be thrown out of the cleaning shoe instantly, but this also increased the possibility of the grain being blown out.

— Under test 5 in Fig. 14e, the airflow velocity was ~ 8.5 m/s at the fan upper duct, which approached the suspension velocity of the grain. Then, the airflow velocity gradually decreased along the sieve length, and the airflow velocity lateral distribution was not uniform in the cleaning shoe. The airflow velocity reached the lowest value at the sieve length of 540-720 mm, and the short straw entered the grain tank and impaired the grain impurity ratio, although the airflow velocity overall distribution was ideal.

— Under test 6 in Fig 14f, the airflow velocity at the fan upper duct was more uniform in the transverse direction, and the averaged airflow velocity was ~ 10 m/s. The short straw can be blown to a far position under the coupling action of the strong airflow from the upper duct and vibrating sieve, as the airflow velocity was larger in the sieve front section. The decreasing airflow velocity in the

Table 2. Experimental cleaning performance under different conditions

Test No.	Fan speed (rpm)	Guide plate I angle (°)	Guide plate II angle (°)	Sieve opening (mm)	Grain sieve loss (%)	Grain impurity ratio (%)
1	1100	8	13	20	0.26	1.03
2	1100	27	29	25	0.42	1.22
3	1100	45	45	30	0.16	2.01
4	1300	8	29	30	0.39	0.76
5	1300	27	45	20	0.69	0.63
6	1300	45	13	25	0.53	1.22
7	1500	8	45	25	1.28	0.94
8	1500	27	13	30	1.80	0.75
9	1500	45	29	20	0.78	1.26

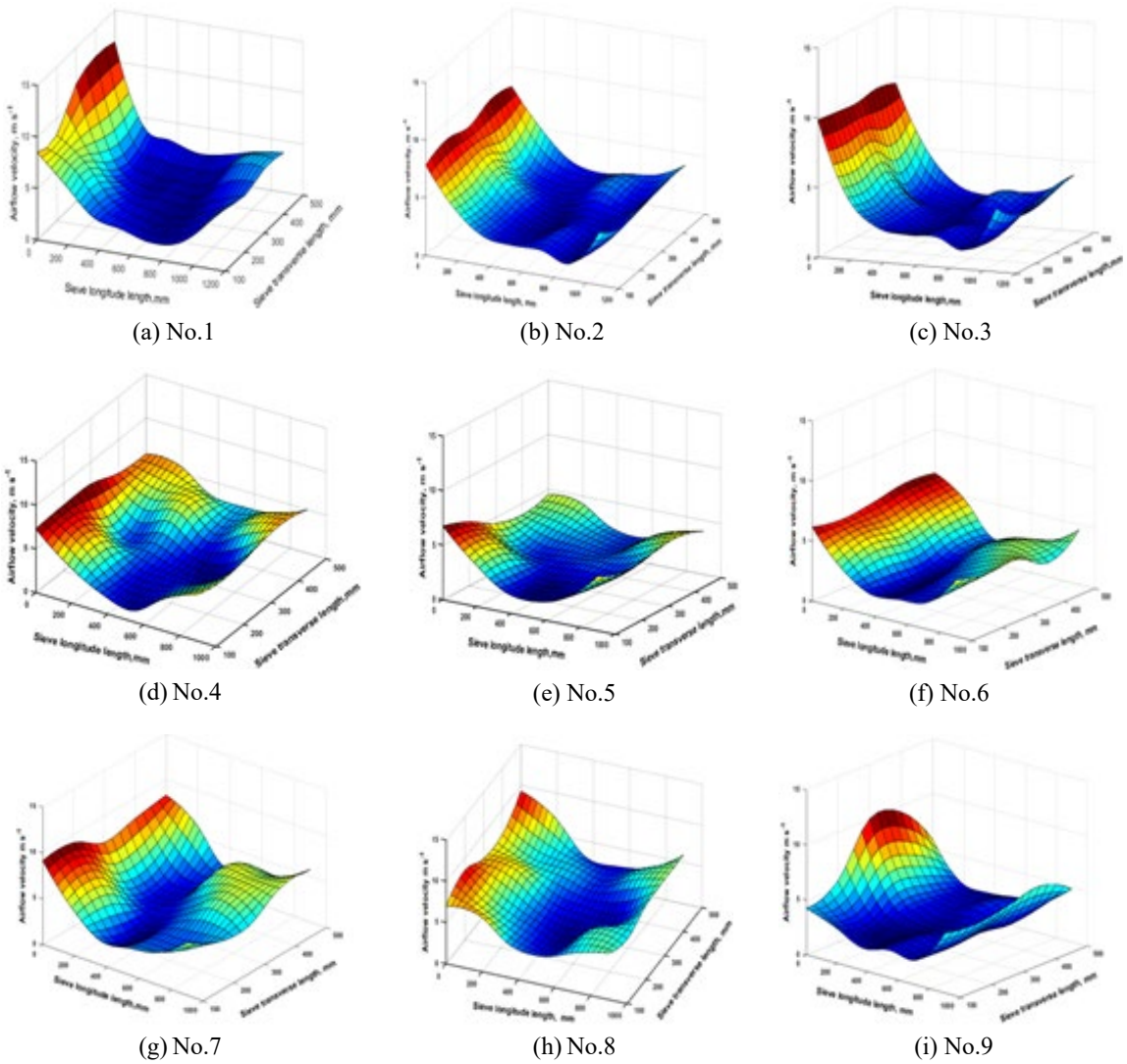

(a) No.1 (b) No.2 (c) No.3

(d) No.4 (e) No.5 (f) No.6

(g) No.7 (h) No.8 (i) No.9

Figure 14. Airflow velocity distribution characteristic above sieve under different conditions

middle section of the sieve and the recovery in the tail sieve were good for improving cleaning performance.

— Under test 7 in Fig 14g, the airflow velocity was more uneven along the sieve width direction, and the airflow velocity fluctuated greatly. Uneven airflow velocity lead to a partial accumulation of threshed outputs on the sieve surface, resulting in airflow turbulence in the cleaning shoe. In addition, the airflow velocity in the front sieve (0-180 mm) was distributed in the range of 8-12 m/s, the grain entering the cleaning shoe at a larger initial velocity under this condition, and the accelerated grains were thrown out, resulting in larger grain sieve loss.

— Under test 8 in Fig. 14h, the airflow velocity was higher in the cleaning shoe than in the other groups, but the airflow velocity experienced considerable lateral fluctuation. The higher airflow velocity at the fan upper duct and tail sieve lead to larger grain sieve loss.

— Under test 9 in Fig 14i, the airflow velocity had an even distribution on the sieve transverse direction in the front sieve, and the averaged airflow velocity was ~ 12.5 m/s. The airflow velocity experienced a drastic decline in the range of 0-180 mm in the sieve length direction, and grains settled into the grain auger promptly. After that, the airflow velocity decreased significantly, and short straw entered the grain auger. Airflow velocity was stable within the range of 720-900 mm in sieve length. The accelerated grains were blown out under the action of strong airflow at the tail sieve, resulting in larger grain sieve loss.

From the above analysis, it can be seen that there was significant airflow velocity fluctuation inside the cleaning shoe, but there was a similar distribution mode along the sieve, that is, the airflow velocity arrived at its largest value at the upper duct, and the airflow velocity at the middle of the sieve (500-900 mm) was the lowest. The airflow velocity recovered to some extent in the tail sieve (900-1080 mm). The airflow velocity in the cleaning shoe is shown in Fig. 15. From the test-rig experiment results, test 4 and test 6 exhibited the best cleaning performance; thus, the desired airflow distribution range is that 8-9 m/s at the upper duct, 4-6 m/s

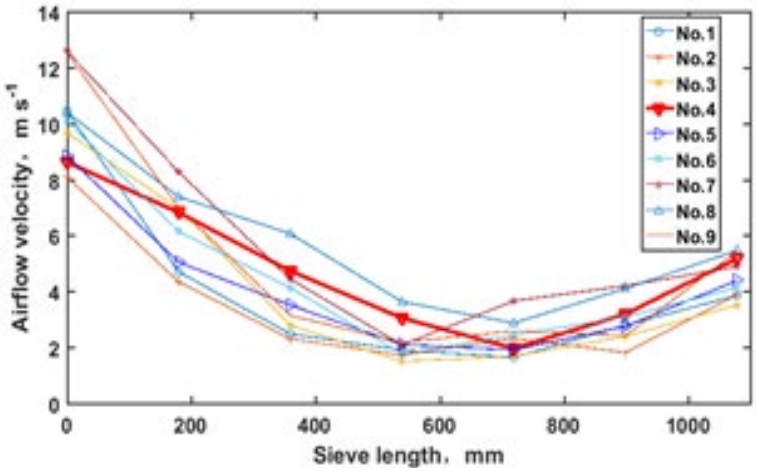

Figure 15. Averaged airflow velocity at different measuring points in cleaning shoe

at the middle section, and 3-4 m/s at the tail section was the ideal airflow velocity distribution. This result verifies that the airflow velocity had a significant relation with cleaning performance.

Field experiment results

The corresponding field experiment results of the combine harvester with the selected multi-duct fan were as follows: the grain sieve loss was 0.23% and the grain impurity ratio 0.41% under a fan speed of 1300 rpm; the guide plate I angle 8°, the guide plate II angle 45°, and the sieve opening 30 mm. The corresponding grain sieve loss was 0.066% and the grain impurity ratio 0.627% when the fan speed was 1100 rpm; the sieve opening 20 mm, the guide plate I angle 8°, and the guide plate II angle 45°.

Conclusion

As the load increases (higher resistance values), the eddy scope and the airflow velocity inside the fan gradually decrease, resulting in a reduced airflow velocity at each duct. Higher airflow velocity at the fan upper duct and tail sieve lead to larger grain sieve loss. The decreasing airflow velocity in the middle section of the sieve and the recovery in the tail sieve were good for improving cleaning performance. In this study, the cleaning system performance was just predicted according to the terminal velocity of the different categories of threshed outputs and airflow velocity magnitude, in the future, CFD-DEM (discrete element method) coupling method can be utilized to study the threshed outputs movements under different fan speed, sieve vibration frequency and airflow direction, thus the cleaning performance can be predicted more precisely though simulation.

References

Adewumi BA, Rao SBV, Kumar KNL, Ventakrishnan L, Karthikeyan L, 2008. Velocity and trajectory profiles of soybean grains in cross flow system. Food Process Automat Conf, Rhode Island, USA, ASABE Publication Number 701P0508cd.

An X, Li Z, Zude-Sasse M, Tchuenbou-Magaia F, Yang Y, 2020. Characterization of textural failure mechanics of strawberry fruit. J Food Eng 282: 110016. https://doi.org/10.1016/j.jfoodeng.2020.110016

Casarsa L, Giannattasio P, 2011. Experimental study of the three-dimensional flow field in cross-flow fans. Exp Thermal Fluid Sci 35 (6): 948-959. https://doi.org/10.1016/j.expthermflusci.2011.01.015

Chen N, Chen DJ, Tian XJ, Tian XJ, Zhang JR, 2009. Theory and experiment on non-uniform air-flow cleaning of air-screen cleaning unit. T CSAM 40 (4): 73-77.

Chinese Academy of Agricultural Mechanization Sciences, 2007. Manual of agricultural machinery design, China Agr Sci Technol Press, Beijing, pp: 963-966.

Dieter B, Jing R, Michael S, 2005. Influence of stator clocking on the unsteady three-dimensional flow in a two-stage turbine, J Turbomach 127 (1): 156-163. https://doi.org/10.1115/1.1812780

Dilin P, Sakai T, Wilson M, Whitfield A, 1998. A computational and experimental evaluation of the performance of a centrifugal fan volute. P I Mech Eng A-J Pow 212: 235-246. https://doi.org/10.1243/0957650981536763

Gao B, Yang L, Zhang N, Du WQ, Yuan X, 2018. Effects of tongue tip radius on performance and hydrodynamic load characteristics in centrifugal pump. J Drain Irrig Mach Eng 36 (3): 185-190, 203.

Gebrehiwot MG, 2010. Computational and experimental analysis of a wide cleaning fan for a harvester, Doctoral thesis. KU Leuven, Leuven, Belgium.

Gebrehiwot MG, De Baerdemaeker J, Baelmans M, 2010a. Effect of a cross-flow opening on the performance of a centrifugal fan in a combine harvester. Biosyst Eng 105: 247-256. https://doi.org/10.1016/j.biosystemseng.2009.11.003

Gebrehiwot MG, De Baerdemaeker J, Baelmans M, 2010b. Numerical and experimental study of a cross-flow fan for combine cleaning shoes. Biosyst Eng 106 (4): 448-457. https://doi.org/10.1016/j.biosystemseng.2010.05.009

Kenney KL, Wright CT, Bryden KM, 2005. Virtual engineering approach to developing selective harvest technologies. ASAE Paper No. 056046. St. Joseph, Mi, USA.

Kergourlay G, Kouidri S, Rankin GW, Rey R, 2006. Experimental investigation of the 3D unsteady flow field downstream of axial fans. Flow Meas Instrum 17 (5): 303-314. https://doi.org/10.1016/j.flowmeasinst.2006.05.002

Li F, Li YM, 2015. Optimization and simulation research of the airway of tangential-axial combine harvester cleaning room. J Agric Mech Res 02: 75-78.

Liang ZW, Li YM, Xu LZ, 2019. Grain sieve loss fuzzy control system in rice combine harvesters. Appl Sci-Basel 9: 114. https://doi.org/10.3390/app9010114

Liang ZW, Xu LZ, De Baerdemaeker J, Li YM, Saeys W, 2020. Optimisation of a multi-duct cleaning device for rice combine harvesters utilising CFD and experiments. Biosyst Eng 190: 25-40. https://doi.org/10.1016/j.biosystemseng.2019.11.016

Molenda M, Montross MD, Mcneill SG, Horabik J, 2005. Airflow resistance of seeds at different bulk density using erguns equation, T ASAE 48 (3): 1137-1145. https://doi.org/10.13031/2013.18487

Muggli FA, Holbein P, Dupont P, 2002. CFD calculation of a mixed flow pump characteristic from shut off to maximum flow. J Fluid Eng-T ASME 124: 798-802. https://doi.org/10.1115/1.1478061

Sakya AE, Yoshiaki N, Michiru Y, 1993. Evaluation of an RNG-based algebraic turbulence model. Comput Fluids 22 (2): 207-214. https://doi.org/10.1016/0045-7930(93)90052-B

Semion S, Boris G, Ilya S, 2003. Cross-term and ε-expansion in RNG theory of turbulence. Fluid Dyn Res 33 (4): 319-331. https://doi.org/10.1016/j.fluiddyn.2003.08.001

Seo SJ, Kim KY, Kang SH, 2003. Calculations of three dimensional viscous flow in a multi-blade centrifugal fan by modeling blade forces. P I Mech Eng A-J Pow 217: 287-297. https://doi.org/10.1243/095765003322066510

Tang CZ, Zhang XY, Ouyang ZH, Luo HF, Fang YX, Wu B, 2007. Experimental research on the combined centrifuge-aerofoil grain cleaning fan. T CSAE 23 (10): 117-120.

Ueka Y, Matsui M, Inoue E, Mori K, Okayasu T, Mitsuoka M, 2012. Turbulent flow characteristics of the cleaning wind in combine harvester. Eng Agric Environ Food 5 (3): 102-106. https://doi.org/10.1016/S1881-8366(12)80022-X

Wu QF, 2014. TC5000 series new combines of New Holland Company. Agric Eng 4 (5): 31-34.

Xu LZ, Alan CH, Li YM, Liang ZW, Yu LJ, 2015. Numerical and experimental analysis of airflow in a multi-duct cleaning system for a rice combine harvester. T ASABE 59 (5): 1101-1110. https://doi.org/10.13031/trans.59.11569

Yuan L.P. 2017. Progress in super-hybrid rice breeding. The Crop J 5 (2):100-102. https://doi.org/10.1016/j.cj.2017.02.001

Zhang JF, Li GD, Mao JY, Yuan SQ, Qu YF, Jia J, 2018. Effects of the outlet position of splitter blade on the flow characteristics in low-specific-speed centrifugal pump. Adv Mech Eng 10 (7): 1-12. https://doi.org/10.1177/1687814018789525

Zhao Z, Huang HD, Yin, JJ, Yang SX, 2018. Dynamic analysis and reliability design of round baler feeding device for rice straw harvest. Biosyst Eng 174: 10-19. https://doi.org/10.1016/j.biosystemseng.2018.06.014